2019 IEEE 58th Conference on Decision and Control (CDC)
Palais des Congrès et des Expositions Nice Acropolis
Nice, France, December 11-13, 2019

Optimal Walking Speed Transitions for Fully Actuated Bipedal Robots*

Vishal Murali[1], Aaron D. Ames[2] and Erik I. Verriest[1]

Abstract— **In this paper, we utilize the Partial Hybrid Zero Dynamics (PHZD) framework to find a continuous family of stable periodic orbits on the PHZD surface. We find optimal controllers to transition between these types of orbits subject to PHZD constraints, along with finding optimal periodic orbits associated to different PHZD surfaces for different walking speeds. Additionally, optimal controllers that form a connecting surface between these distinct PHZD surfaces, along with transitions between them are synthesized. The two methods are compared with performance metrics associated with the cost of transport. The results are illustrated on a 5 degree of freedom planar bipedal robot.**

I. INTRODUCTION

The problem of transitioning between different walking speeds and more generally gait transitions has been widely studied by researchers. Understanding how to transition between gaits is important for achieving efficiency in locomotion and for high level motion planning of legged robots. The ability to modulate speed on walking robots in an optimal fashion will be an important component to realizing walking robots in a variety of real-world settings.

One of the widely used approaches to motion planning and control of bipedal robots is the Zero Moment Point (ZMP) planning approach [1],[2]. ZMP methods involve generating a foot step plan, a foot step compatible ZMP plan and subsequently a center of mass plan using linear inverted pendulum models and using inverse kinematics to get the reference joint trajectories. Subsequently, lower level controllers can be used to track these joint references. Hence ZMP methods can be used naturally for rapid motion planning and for obstacle avoidance. More general centroidal momentum models are used in [3]. However a drawback of these methods is that the resulting gaits and transitions do not use full dynamics and have lower energy efficiency.

Several researchers have focused on transitions between dynamic walking/running gaits. A popular approach to transitions is the construction of motion primitives and sequential composition of motion primitives. Funnel based switching between limit cycles in a Spring Loaded Inverted Pendulum (SLIP) model of running was accomplished in [4] with touch down angle control, hip and prismatic actuators. A two step deadbeat control for transitioning between equilibrium gaits (periodic orbits) was obtained for SLIP using touch down angle control [5]. A method for the generation of a continuous family of limit cycles on a continuous family of Hybrid Zero Dynamics (HZD) surfaces was obtained in [6]. A switching control law is then used in [6] to achieve walking speed transitions. Funnel based switching of HZD controllers for navigation and obstacle avoidance of bipedal robots was achieved in [7] by estimating Region of Attraction. An orbit library is constructed in [8], wherein each fixed orbit is stabilized by trajectories transitioning from other orbits in the library to the fixed orbit. [9] transitions between motion primitives for navigation on uneven terrain. However, these approaches do not transition between gaits in an *optimal* manner.

This paper focuses specifically on transitions between periodic orbits of different walking speeds for a fully actuated bipedal robot. We utilize the *partial hybrid zero dynamics* [10],[11] framework to generate a partial zero dynamics surface $PZ_{\alpha(v_f)}$ and an infinite family of periodic orbits $\mathcal{O}(v_d, \alpha(v_f))$ on $PZ_{\alpha(v_f)}$ of different walking speeds v_d. Following the development of [11] we have a reduced order two dimensional controlled hybrid system that allows us to transition between any of these orbits on $PZ_{\alpha(v_f)}$. We formulate and solve an *optimal control problem* to transition between these types of orbits subject to staying in the partial zero dynamics surface $PZ_{\alpha(v_f)}$ which is one of the main contributions of this paper. The surface $PZ_{\alpha(v_f)}$ is obtained by optimizing a performance index $\mathcal{J}_1(\alpha, v_f)$ (see III-B) with respect to α for a fixed v_f. Therefore, the family of periodic orbits $\mathcal{O}(v_d, \alpha(v_f))$ on $PZ_{\alpha(v_f)}$ need not be optimal with respect to $\mathcal{J}_1(\alpha, v_d)$ for $v_d \neq v_f$. We therefore optimize for different surfaces $PZ_{\alpha(v_d)}$ for several (discrete) walking speeds v_d. Since these periodic orbits are on different partial zero dynamics surfaces, we construct a controlled invariant surface $PZ_{\beta(v_1,v_2)}$ that connects distinct surfaces $PZ_{\alpha(v_1)}$ and $PZ_{\alpha(v_2)}$.

A similar approach to the results presented was taken in [12] where they used an extended canonical walking function to connect two different (optimized) PHZD surfaces. The coefficients of the extended canonical walking function were obtained in closed form based on the boundary conditions to connect the two distinct PHZD surfaces. In contrast, we solve an *optimization problem* to connect two different PHZD surfaces. This is advantageous (although computationally more burdensome) as we can not only optimize for efficiency, but also explicitly include all the physical modeling constraints of the robot during transition which [12] does not explicitly guarantee. This is the second contribution of this paper. Finally, we compare all the transition controllers used in this paper with a uniform performance index related to the cost of transport. This is demonstrated in simulation.

*This work was supported by NSF grant CPS1544857

[1]The authors are with The School of Electrical and Computer Engineering, Georgia Institute of Technology, Atlanta, GA, 30332 vmurali8@gatech.edu, erik.verriest@ece.gatech.edu

[2] The author is Bren Professor at Caltech ames@caltech.edu

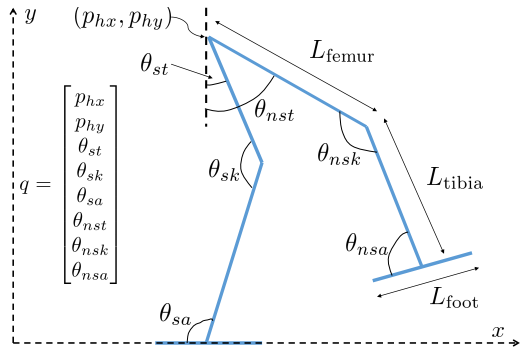

Fig. 1: Schematic of the planar 5 DOF walking robot

II. Walking Robot Model

We discuss the robot model used throughout this paper. The robot has five degrees of freedom and is fully actuated as shown in Fig 1. The robot has only a single support phase, where the non stance foot is above the ground and the stance foot is flat on the ground. We assume that the non-stance foot impacts flat on the ground. Once the non-stance foot impacts in elastically on the ground, it is assumed that the non stance foot has zero velocity and hence becomes the current stance foot. The prior stance foot then becomes the non-stance foot and has positive vertical velocity. We thus relabel legs after impact to label the non stance leg prior impact as the stance leg after impact and vice-versa for the stance leg. With these modeling assumptions, we can define a hybrid system model of the robot by [13]

$$\mathcal{H} = (\mathcal{D}, \mathcal{G}, \Delta, f, g) \tag{1}$$

The details of of $\mathcal{H}$ are provided below.

A. Robot Dynamics

We use floating base coordinates of the walking robot as shown in Fig 1. The configuration space $Q = \mathbb{R}^2 \times \mathbb{S}^6$. Local coordinates for Q are depicted in Fig 1. The function defining the holonomic constraints is given as follows

$$h(q) = \begin{bmatrix} p^{\text{com}}_{\text{sfx}}(q) \\ p^{\text{com}}_{\text{sfy}}(q) \\ \theta_{\text{sf}}(q) \end{bmatrix} \tag{2}$$

where $q \in \mathbb{R}^8$, $p^{\text{com}}_{\text{sfx}}(q) \in \mathbb{R}$, $p^{\text{com}}_{\text{sfy}}(q) \in \mathbb{R}$ denote the (global) horizontal and vertical position and $\theta_{\text{sf}}(q)$ is the global orientation of the stance foot link with respect to the horizontal. In the single support phase, the stance foot is flat on the ground, so $p^{\text{com}}_{\text{sfx}}(q) = \text{constant}$, $p^{\text{com}}_{\text{sfy}}(q) = 0$ and $\theta_{\text{sf}}(q) = 0$ are the holonomic constraints. Symbolic closed form expressions for $h(q)$ can be obtained from the forward kinematics. The equations of motion for the robot in floating base coordinates can be written as

$$M(q)\ddot{q} + C(q,\dot{q})\dot{q} + G(q) = Bu + \frac{\partial h}{\partial q}^{\top} \lambda \tag{D1}$$

$$\frac{\partial h}{\partial q}\ddot{q} + \frac{d}{dt}\left(\frac{\partial h}{\partial q}\right)\dot{q} = 0 \tag{D2}$$

$M(q) \in \mathbb{R}^{8\times 8}$ is the inertia matrix. $\lambda \in \mathbb{R}^3$ are *forces of constraint* which can be explicitly obtained by substituting $\ddot{q}$ from (D1) into (D2). $B \in \mathbb{R}^{8\times 5}$ is a (full rank) matrix that maps joint torques to generalized forces. (D1) - (D2) represent the continuous dynamics of the robot. The non stance foot impacts corresponds to a relabeling in the configuration space

$$q^+ = Rq^- \tag{3}$$

R is a relabeling matrix that does not change the global coordinates and $R^2 = I$. The post-impact joint velocity can be obtained from the pre-impact joint velocity by solving

$$\begin{bmatrix} M(q) & -\frac{\partial p^{\text{com}}_{\text{nsf}}}{\partial q}^{\top} \\ \frac{\partial p^{\text{com}}_{\text{nsf}}}{\partial q}(q) & 0 \end{bmatrix} \begin{bmatrix} v^+ \\ \delta\lambda \end{bmatrix} = \begin{bmatrix} M(q)\dot{q}^- \\ 0 \end{bmatrix} \tag{4}$$

as in [14]. We then have to relabel the post-impact joint velocities as

$$\dot{q}^+ = Rv^+ \tag{5}$$

Hence the full reset map can be represented as a function

$$(q^+, \dot{q}^+) = \Delta(q^-, \dot{q}^-) \tag{6}$$

where Δ is obtained from (3)-(5). The domain of the single support phase can be formally represented as

$$\mathcal{D} = \left\{ (q,\dot{q}) \in TQ \middle| p^{\text{left}}_{\text{nsfy}}(q) \geq 0, p^{\text{right}}_{\text{nsfy}}(q) \geq 0 \right\} \tag{7}$$

where $p^{\text{left}}_{\text{nsfy}}(q)$ ans $p^{\text{right}}_{\text{nsfy}}(q)$ represent the vertical position of the left end and right end of the non stance foot link. The Guard Set can be represented as

$$\mathcal{G} = \left\{ (q,\dot{q}) \in TQ \middle| p^{\text{com}}_{\text{nsfy}}(q) = 0, dp^{\text{com}}_{\text{nsfy}}(q)\dot{q} < 0 \right\} \tag{8}$$

By eliminating λ from (D1) - (D2) and converting the resulting 2nd order ODE to an equivalent 1st order ODE, the affine control system representing the forward evolution can be obtained as:

$$\dot{x} = f(x) + g(x)u \tag{9}$$

where $x = (q, \dot{q}) \in TQ \subset \mathbb{R}^{16}$ is the full state.

B. Contact Forces

In order for the model described earlier to be valid, the stance foot must remain flat on the ground and not slip. This imposes constraints on the contact forces. From the definition of the holonomic constraints given in (2) we see that $\lambda(1)$ represents the total (tangential) frictional force on the robot, $\lambda(2)$ is the total normal force exerted by the ground on the robot and $\lambda(3)$ is the net moment exerted by the ground contact forces on the stance foot center of mass. Since the stance foot is not slipping, the friction cone constraint must be satisfied

$$-\mu\lambda(2) \leq \lambda(1) \leq \mu\lambda(2). \tag{D3}$$

Also the total normal force must be positive

$$\lambda(2) \geq 0. \tag{D4}$$

Since the stance foot is not rotating the *Zero Moment Point (ZMP) constraint* must be satisfied [14]:

$$-\frac{L_{\text{foot}}}{2}\lambda(2) \leq \lambda(3) \leq \frac{L_{\text{foot}}}{2}\lambda(2) \tag{D5}$$

where L_{foot} is the total length of the foot. If the ZMP constraint is violated the stance foot rotates and our assumption that the robot is fully actuated is no longer valid.

III. Partial Hybrid Zero Dynamics Optimization

We discuss in this section the optimization problem involved in finding a continuous family of stable periodic orbits, based on the PHZD framework. We first discuss about the controller design and then we discuss the optimization problem involved.

A. Controller Design

The controller on the robot seeks to drive certain outputs to zero as we now describe. We define

$$z_1(q) = p_{hx} - p^{\text{com}}_{\text{sfx}}(q) \tag{10}$$

to be the horizontal displacement of the hip with respect to stance foot center of mass. We have the relative degree one output

$$y_1(q, \dot{q}, v_f) = z_2(q, \dot{q}) - v_f \tag{11}$$

where $z_2(q, \dot{q})$ represents the hip velocity given by

$$z_2(q, \dot{q}) = \frac{\partial z_1}{\partial q}(q)\dot{q} \tag{12}$$

and $v_f \in \mathbb{R}$ represents a desired fixed walking speed. The (vector) relative degree two outputs are

$$y_2(q) = y^a(q) - y^d(\tau(q), \alpha) \tag{13}$$

where $y^a(q)$ represents the "actual outputs" given by

$$y^a(q) = \begin{bmatrix} \frac{\pi}{2} + \theta_{nst} - \theta_{nsk} + \theta_{nsa} \\ \theta_{sk} \\ \theta_{nst} - \theta_{st} \\ \theta_{nsk} \end{bmatrix} \tag{14}$$

and $y^d(t, \alpha)$ represent the desired outputs given by bezier polynomials

$$y^d(t, \alpha) = \sum_{k=1}^{M} \alpha_k \frac{M!}{k!(M-k)!} t^k (1-t)^{M-k} \tag{15}$$

where each α_k is a 4×1 vector and $\alpha = \{\alpha_k\}_{k=1}^M$ is a column vector of all the α_k stacked together and the parameter $M = 6$. $\tau(q)$ is monotonic throughout a step and is known as the phase variable and is given by

$$\tau(q) = \frac{z_1(q) - z_1^+}{z_1^- - z_1^+} \tag{16}$$

where the parameters z_1^+ and z_1^- are chosen to ensure that $\tau(q) \in [0, 1]$ throughout a step, i.e., they are chosen based upon the initial and final position of the robot during a step. With these outputs the feedback control

$$u_\epsilon(q, \dot{q}, \alpha, v_f) = \mathcal{A}_\alpha^{-1}(q, \dot{q}) \left(\begin{bmatrix} 0 \\ L_f^2 y_2(q, \dot{q}) \end{bmatrix} + \begin{bmatrix} L_f z_2(q, \dot{q}) \\ 2\epsilon L_f y_2(q, \dot{q}) \end{bmatrix} + \begin{bmatrix} \epsilon\left(z_2(q, \dot{q}) - v_f\right) \\ \epsilon^2 y_2(q) \end{bmatrix} \right) \tag{17}$$

where the decoupling matrix

$$\mathcal{A}_\alpha(q, \dot{q}) = \begin{bmatrix} L_g z_2(q, \dot{q}) \\ L_g L_f y_2(q, \dot{q}, \alpha) \end{bmatrix} \tag{18}$$

yields the output dynamics

$$\dot{y}_1 + \epsilon y_1(q, \dot{q}, v_f) = 0 \tag{O1}$$

$$\ddot{y}_2 + 2\epsilon \dot{y}_2(q, \dot{q}, \alpha) + \epsilon^2 y_2(q, \alpha) = 0 \tag{O2}$$

Because we have rendered these dynamics stable, the solutions converge to the (1-dimensional) surface defined by these functions being identically zero, i.e., to the *full zero dynamics* surface:

$$FZ_\alpha = \Big\{ (q, \dot{q}) \in TQ \Big| y_1(q, \dot{q}, v_f) = 0, \; y_2(q, \alpha) = \dot{y}_2(q, \dot{q}, \alpha) = 0 \Big\} \tag{19}$$

We are interested in varying the desired velocity, v_f, and thus we wish to consider the surface where the output y_1 is allowed to vary but the output y_2 is identically zero. This is termed the *partial zero dynamics* surface and given by:

$$PZ_\alpha = \Big\{ (q, \dot{q}) \in TQ \Big| y_2(q, \alpha) = \dot{y}_2(q, \dot{q}, \alpha) = 0 \Big\} \tag{20}$$

The control given by (17) renders both FZ_α and PZ_α forward invariant. However, in the presence of impacts, we only enforce invariance of PZ_α as discussed in the optimization problem below. We note that on PZ_α, the dynamics of the system

$$\dot{x} = f(x) + g(x) u_\epsilon(x, \alpha, v_f) \tag{21}$$

can be represented by a second order system

$$\begin{aligned} \dot{z}_1 &= z_2 \\ \dot{z}_2 &= -\epsilon(z_2 - v_f) \end{aligned} \tag{22}$$

and the state $(q, \dot{q})$ can be reconstructed as

$$(q, \dot{q}) = (\phi_{PZ}(z_1), \psi_{PZ}(z_1) z_2) \tag{23}$$

Finally, we note that given $(z_1^-, z_2^-) \in \mathcal{G} \cap PZ_\alpha$, we can obtain the equivalent $(q^-, \dot{q}^-) \in \mathcal{G} \cap PZ_\alpha$ according to (23), then apply the reset map to obtain $(q^+, \dot{q}^+) = \Delta(q^-, \dot{q}^-)$ and finally $(z_1^+, z_2^+) = (z_1(q^+), z_2(q^+, \dot{q}^+))$ where $z_1(q)$ and $z_2(q, \dot{q})$ are given in (10) and (12). We thus obtain:

$$\left(z_1^+, z_2^+\right) = \Delta_{PZ}\left(z_1^-, z_2^-\right) \tag{24}$$

We have thus constructed a reduced order two dimensional hybrid system (assuming (N1)) inside the full hybrid system with continuous dynamics given by (22) and reset map given by (24).

B. Optimization

With the controller design in place, we now discuss an optimization problem to find a PZ_α that contains a periodic orbit that is optimal with respect to a prescribed performance index, subject to physical constraints. The performance index is motivated by the cost of transport and is taken as

$$\mathcal{J}_1 = \frac{1}{mgd}\int_0^T u^\top u \; dt \tag{25}$$

where m is the total mass of the robot, g is the acceleration due to gravity and d is the step length, i.e the total horizontal distance traveled by the non stance foot over a step. We also would like to obtain parameters α satisfying

$$\Delta(\mathcal{G} \cap PZ_\alpha) \subset PZ_\alpha \tag{N1}$$

This makes the partial zero dynamics surface hybrid invariant, thereby creating *partial hybrid zero dynamics* (PHZD). As discussed in [10], we only enforce impact invariance of the relative degree two outputs, since there is a discontinuous change in the cartesian velocities of the links across impacts. In contrast, the cartesian positions of the links are always continuous. We thus allow for change in the relative degree one outputs (which is the hip velocity) to account for this. To ensure the trajectory begins in PZ_α we enforce

$$y_2(q(0),\alpha) = \dot{y}_2(q(0),\dot{q}(0),\alpha) = 0 \tag{N2}$$

We also have the boundary condition

$$(q(T^-),\dot{q}(T^-)) \in \mathcal{G} \tag{N3}$$

i.e the switching surface is reached at the end of a step. Finally, we also have domain constraints which are inequality constraints

$$(q(t),\dot{q}(t)) \in \mathcal{D}, t \in [0,T] \tag{N4}$$

The optimization problem solved is

$$\begin{aligned} &\min_{\alpha} \mathcal{J}_1(\alpha, v_f) \\ &s.t. \;\; \text{(D1)} - \text{(D5)}, \text{(O1)} - \text{(O2)}, \text{(N1)} - \text{(N4)} \end{aligned} \tag{26}$$

Note that we did not explicitly enforce periodicity constraints, however by [10] for large ϵ in (17) there will be a stable periodic orbit in PZ_α. The end result of the optimization problem is a set of coefficients α that result in stable walking. We denote the solution as $\alpha(v_f)$ and the resulting surface as $PZ_{\alpha(v_f)}$ henceforth.

IV. Transitions between Orbits

In this section, we first discuss transitions between periodic orbits that live on a fixed surface $PZ_{\alpha(v_f)}$ where v_f is a fixed desired walking speed. Subsequently, we discuss transitions between periodic orbits that are in distinct PHZD surfaces.

A. Transitions between orbits on same PHZD

We assume that we can solve (26) for a user defined fixed v_f obtaining a fixed optimal $\alpha(v_f)$ and hence a PHZD surface $PZ_{\alpha(v_f)}$. However, by results of [10], we get an infinite family of stable periodic orbits on $PZ_{\alpha(v_f)}$ for different values of walking speeds v_d (which replaces v_f in (11) but $\alpha(v_f)$ in (13) is fixed as before). We denote such periodic orbits by $\mathcal{O}(v_d, \alpha(v_f))$. We now discuss an optimization formulation to transition between these infinite family of periodic orbits, all living in the fixed surface $PZ_{\alpha(v_f)}$.

To obtain transitions, we use the feedback control given by (17) where $v_f \in \mathbb{R}$ is replaced by a function of time $v_d(t)$ which result in the dynamics on $PZ_{\alpha(v_f)}$ given by

$$\begin{aligned} \dot{z}_1 &= z_2 \\ \dot{z}_2 &= -\epsilon(z_2 - v_d(t)) \end{aligned} \tag{T1}$$

where the full state can still be reconstructed according to (23). Hence, (T1) can be viewed as a *controlled hybrid system* [11] with control input $v_d(t)$ where the reset map is still given by (24). This control input enables us to transition between any two periodic orbits on $PZ_{\alpha(v_f)}$, while still staying in $PZ_{\alpha(v_f)}$. We want to transition between orbits in N steps in an optimal manner, where N is a user defined parameter. We formulate the objective function

$$\mathcal{J}_2 = \frac{1}{mgd_{\text{total}}}\int_{t_0}^{t_N} \phi(t)\, dt \tag{27}$$

where N represents the number of steps in the transitions, d_{total} represents the total horizontal distance traveled by the non stance foot over N steps, and $\phi(t)$ represents the control effort given by

$$\phi(t) = u_{\alpha(v_f)}(z_1(t), z_2(t), v_d(t))^\top u_{\alpha(v_f)}(z_1(t), z_2(t), v_d(t)) \tag{28}$$

The control $u_{\alpha(v_f)}(z_1(t), z_2(t), v_d(t))$ is obtained from (23) and (17). The states $(z_1(t), z_2(t))$ are continuous at all times except at a discrete set of times denoted $\{t_k\}$, $1 \le k \le N$. At these impact times we need to have the discrete reset map

$$\begin{bmatrix} z_1(t_k^+) \\ z_2(t_k^+) \end{bmatrix} = \Delta_{PZ}\left(\begin{bmatrix} z_1(t_k^-) \\ z_2(t_k^-) \end{bmatrix}\right) \tag{T2}$$

We also impose continuity of $v_d(t)$ at the points of impact, namely

$$v_d(t_k^+) = v_d(t_k^-) \tag{T3}$$

for $0 \le k \le N$ where $v_d(t_0^-) = v_1$ represents the initial walking speed and $v_d(t_N^+) = v_2$ represents final walking speed. We also impose the boundary conditions ensuring we start at the initial orbit and end at the final orbit.

$$\begin{aligned} (z_1(t_0), z_2(t_0)) &\in \mathcal{O}(v_1, \alpha(v_f)) \\ \left(z_1(t_N^+), z_2(t_N^+)\right) &\in \mathcal{O}(v_2, \alpha(v_f)) \end{aligned} \tag{T4}$$

Hence, the overall optimization problem solved is

$$\begin{aligned} &\min_{v_d(t)} \mathcal{J}_2(v_d(t)) \\ &s.t \;\; \text{(T1)} - \text{(T4)} \end{aligned} \tag{29}$$

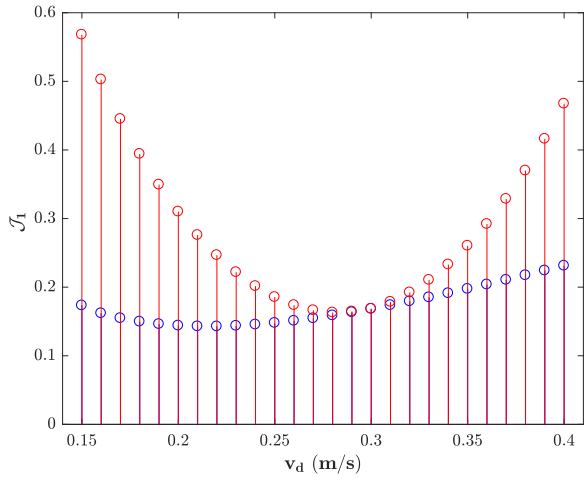

Fig. 2: Comparison of objective function $\mathcal{J}_1$ for the periodic orbits $\mathcal{O}(v_d, \alpha(v_d))$ i.e. $\mathcal{J}_1(u_{\alpha(v_d)}(z_1, z_2, v_d))$ (blue) and $\mathcal{O}(v_d, \alpha(v_f)) \subset PZ_{\alpha(v_f)}$ i.e. $\mathcal{J}_1(u_{\alpha(v_f)}(z_1, z_2, v_d))$ (red) respectively. $v_f = 0.3$ m/s is fixed.

Remark 1: We note that since (T1) is an exponentially stable linear system, appropriately ramping $v_d(t)$ from v_1 to v_2 will effect a transition from $O(v_1, \alpha(v_f))$ to a neighborhood of $O(v_2, \alpha(v_f))$ in N steps and it would do so exponentially fast. However, it is not *optimal* with respect to $\mathcal{J}_2(v_d(t))$ which we illustrate in the subsequent sections.

B. Transition between orbits on different PHZD surfaces

The periodic orbit $\mathcal{O}(v_f, \alpha(v_f)) \subset PZ_{\alpha(v_f)}$ is optimal w.r.t $\mathcal{J}_1(\alpha, v_f)$ by definition of $\alpha(v_f)$ in IV-A. However, the orbits $\mathcal{O}(v_d, \alpha(v_f)) \subset PZ_{\alpha(v_f)}$ are not optimal for $\mathcal{J}_1(\alpha, v_d)$ where $v_d \neq v_f$. This motivates optimizing several PHZD surfaces PZ_α for various walking speeds v_d and constructing transition controllers between them.The periodic orbits on these surfaces are denoted by $\mathcal{O}(v_1, \alpha(v_1))$ and $\mathcal{O}(v_2, \alpha(v_2))$. We connect $PZ_{\alpha(v_1)}$ and $PZ_{\alpha(v_2)}$ over a single step. The objective function used is given by $\mathcal{J}_1$ given in (25) where u is given in (17) is a function of β (the bezier coefficients) and $v_d(t)$. This means that on the connecting surface PZ_β, the dynamics evolve as in (T1). However, the constraint (N1) is replaced by

$$\begin{aligned} &\Delta(\mathcal{G} \cap PZ_{\alpha(v_1)}) \subset PZ_\beta \\ &\Delta(\mathcal{G} \cap PZ_\beta) \subset PZ_{\alpha(v_2)} \end{aligned} \tag{TR1}$$

The optimization problem solved is

$$\begin{aligned} &\min_{\beta, v_d(t)} \ \mathcal{J}_1(\beta, v_d(t)) \\ s.t \ \ &\text{(D1)} - \text{(D5)}, \text{(O1)} - \text{(O2)}, \text{(TR1)}, \text{(N3)} - \text{(N4)} \end{aligned} \tag{30}$$

Optimizing (30) results in a (optimized connecting) PHZD surface denoted $PZ_{\beta(v_1, v_2)}$.

V. Results

This section provides the simulation results for the 5 DOF robot explained in Section II. We first compare the performance index $\mathcal{J}_1$ of the orbits $\mathcal{O}(v_d, \alpha(v_f))$ i.e., $\mathcal{J}_1(u_{\alpha(v_f)}(z_1, z_2, v_d))$ and the periodic orbits $\mathcal{O}(v_d, \alpha(v_d))$ i.e, $\mathcal{J}_1(u_{\alpha(v_d)}(z_1, z_2, v_d))$ for different values of v_d. In this paper, we chose $v_f = 0.3\ m/s$ and solved (26) to obtain $PZ_{\alpha(v_f)}$. The performance index of these orbits is shown in red in Fig 2. We also solved (25) for different v_d to obtain the orbits $O(v_d, \alpha(v_d))$ shown in blue in Fig 2. We see that the performance index $\mathcal{J}_1$ for $\mathcal{O}(v_d, \alpha(v_f))$ gets larger as v_d further deviates from v_f.

1) Definition of Performance Index: In this paper, all the controllers are designed to achieve transitions in $N = 3$ steps. The performance index used is

$$\mathcal{J}_2 = \frac{1}{mgd_{\text{total}}} \int_0^T u^\top u \ dt \tag{31}$$

where d_{total} is the total step length of the robot. Here $[0, T]$ is defined such that it is exactly the duration of *five* steps of the robot, the first step being the initial periodic orbit, the subsequent three steps being the transitions and the fifth step being the final orbit. The motivation for including one step of the initial and final orbit in the performance index calculation is to enable us to compare transitions $\mathcal{O}(v_1, \alpha(v_f)) \rightarrow \mathcal{O}(v_2, \alpha(v_f))$ and $\mathcal{O}(v_1, \alpha(v_1)) \rightarrow \mathcal{O}(v_2, \alpha(v_2))$.

A. Comparison between Transition Controllers on $PZ_{\alpha(v_f)}$

In Remark 1 in IV-A, we stated that we could use a linear ramp to transition between $\mathcal{O}(v_1, \alpha(v_f))$ and $\mathcal{O}(v_2, \alpha(v_f))$ since the dynamics of the robot on $PZ_{\alpha(v_f)}$ is an exponentially stable system given by (T1). That is given initial and final velocities v_1 and v_2, the control input is $v_d^1(t) = c_1 t + c_2$ is applied to the system (T1) such that at time $t = t_i$ we have $v_d^1(t_i) = v_1$ and after three steps of transitions we have $v_d^1(t_f) = v_2$ where $[t_i, t_f]$ is the transition duration. The full control is given by $u_1(t) = u_{\alpha(v_f)}(z_1, z_2, v_d^1(t))$ where $z_1(t)$ and $z_2(t)$ are the solutions of (T1) with v_d^1 as a control input.

Solving (29) gives the optimal input denoted $v_d^2(t)$ that transfers the system from $O(v_1, \alpha(v_f))$ to $\mathcal{O}(v_2, \alpha(v_f))$ subject to being in $PZ_{\alpha(v_f)}$ in 3 steps. Given the control $v_d^2(t)$, we can get the full control $u_2(t) = u_{\alpha(v_f)}(z_1, z_2, v_d^2(t))$. The performance index $\mathcal{J}_2$ given in (31) is evaluated on both u_1 and u_2. The results are illustrated in Table I. We see that for increasing transitions ($v_1 < v_2$), there is a lot of improvement when the gap between $v_2 - v_1$ is small but it decreases with increasing gap between $v_2 - v_1$. For decreasing transitions ($v_1 > v_2$). In all cases the performance improvement is larger than 5 percent.

B. Comparison between Optimal Transition Controllers on $PZ_{\alpha(v_f)}$ and Transition Controllers connecting different PHZD surfaces

We obtain one step optimal controllers to transition between orbits $\mathcal{O}(v_1, \alpha(v_1)) \subset PZ_{\alpha(v_1)}$ and $\mathcal{O}(v_2, \alpha(v_2)) \subset PZ_{\alpha(v_2)}$ by solving (30) to obtain $\beta(v_1, v_2)$ and a $v_d(t)$. The full control over one step is then $u_{\beta(v_1, v_2)}(z_1, z_2, v_d(t))$ We then compose these controllers to obtain multi step transitions. For example, to obtain a transition $0.15 \rightarrow 0.30$ m/s, we obtain *one step* transition controllers $0.15 \rightarrow 0.20$ m/s ,

TABLE I: Comparison of Performance Metrics for 3 step Transition Controllers

Walking Speed Transition	Performance Index			Performance Improvement	
	$\mathcal{J}_2(u_1)$	$\mathcal{J}_2(u_2)$	$\mathcal{J}_2(u_3)$	$\frac{\mathcal{J}_2(u_1)-\mathcal{J}_2(u_2)}{\mathcal{J}_2(u_1)} \times 100$	$\frac{\mathcal{J}_2(u_2)-\mathcal{J}_2(u_3)}{\mathcal{J}_2(u_2)} \times 100$
$0.15 \rightarrow 0.20$ m/s	0.9862	0.7062	0.3033	28.3908	57.0518
$0.15 \rightarrow 0.22$ m/s	0.9687	0.7297	0.3544	24.6650	51.4321
$0.15 \rightarrow 0.24$ m/s	0.9864	0.7849	0.4138	20.4228	47.2799
$0.15 \rightarrow 0.26$ m/s	1.0351	0.8662	0.4993	16.3183	42.3574
$0.15 \rightarrow 0.28$ m/s	1.1123	0.9791	0.5961	11.9716	39.1176
$0.15 \rightarrow 0.30$ m/s	1.2244	1.1251	0.7116	8.1151	36.7523
$0.30 \rightarrow 0.25$ m/s	0.3346	0.3149	0.2681	5.8885	14.8619
$0.30 \rightarrow 0.23$ m/s	0.3835	0.3509	0.3101	8.5029	11.6272
$0.30 \rightarrow 0.21$ m/s	0.4444	0.4128	0.3519	7.1226	14.7529
$0.30 \rightarrow 0.19$ m/s	0.5327	0.4962	0.4324	6.8565	12.8577
$0.30 \rightarrow 0.17$ m/s	0.6540	0.6026	0.5308	7.8580	11.9150
$0.30 \rightarrow 0.15$ m/s	0.7989	0.7311	0.6434	8.4821	11.9956

$0.20 \rightarrow 0.25$ m/s and $0.25 \rightarrow 0.30$ m/s and execute these controllers one after the other. The resulting net transition controller (over all the three steps) is denoted $u_3(t)$ and the corresponding reduced controller is $v_d^3(t)$. The resulting performance index $\mathcal{J}_2$ given in (31) is evaluated to obtain $\mathcal{J}_2(u_3)$. This approach was followed for several different cases and is illustrated in Table I. We see that for increasing transitions there is a tremendous improvement of $\mathcal{J}_2(u_3)$ over $\mathcal{J}_2(u_2)$. The reason is because u_2 attempts to transition from $\mathcal{O}(v_1, \alpha(v_f)) \rightarrow \mathcal{O}(v_2, \alpha(v_f))$. But $\mathcal{O}(v_1, \alpha(v_f))$ has a very high performance index $\mathcal{J}_1$ for $v_1 = 0.15$ m/s (see Fig 2). On the other hand $v_f = 0.30$ m/s so for decreasing transitions ($0.30 \rightarrow 0.15$ m/s for example) the performance improvement is comparatively lower. In all cases the improvement was over 11.91 percent.

VI. Conclusion

In this paper we utilized the partial hybrid zero dynamics framework to generate an infinite family of periodic orbits of different walking speeds on a fixed surface. We then obtain optimal controllers to transition between these orbits. These controllers are compared with a naive linear ramp (which also achieves transitions) to demonstrate their effectiveness. We also show that these different orbits on a given PHZD surface are not themselves optimal. We therefore obtain optimal controllers to transition between optimal periodic orbits. This is also compared and shown to do better than the previous two families of controllers.

References

[1] S. Kajita, F. Kanehiro, K. Kaneko, K. Fujiwara, K. Harada, K. Yokoi, and H. Hirukawa, "Biped walking pattern generation by using preview control of zero-moment point," in *2003 IEEE International Conference on Robotics and Automation (Cat. No. 03CH37422)*, vol. 2. IEEE, 2003, pp. 1620–1626.

[2] S. Kuindersma, F. Permenter, and R. Tedrake, "An efficiently solvable quadratic program for stabilizing dynamic locomotion," in *2014 IEEE International Conference on Robotics and Automation (ICRA)*. IEEE, 2014, pp. 2589–2594.

[3] Y. Zhao, B. R. Fernandez, and L. Sentis, "Robust optimal planning and control of non-periodic bipedal locomotion with a centroidal momentum model," *The International Journal of Robotics Research*, vol. 36, no. 11, pp. 1211–1242, 2017.

[4] P. A. Bhounsule, A. Zamani, and J. Pusey, "Switching between limit cycles in a model of running using exponentially stabilizing discrete control lyapunov function," in *2018 Annual American Control Conference (ACC)*. IEEE, 2018, pp. 3714–3719.

[5] H. R. Vejdani, A. Wu, H. Geyer, and J. W. Hurst, "Touch-down angle control for spring-mass walking," in *2015 IEEE International Conference on Robotics and Automation (ICRA)*. IEEE, 2015, pp. 5101–5106.

[6] S. Veer, M. S. Motahar, and I. Poulakakis, "Generation of and switching among limit-cycle bipedal walking gaits," in *2017 IEEE 56th Annual Conference on Decision and Control (CDC)*. IEEE, 2017, pp. 5827–5832.

[7] M. S. Motahar, S. Veer, and I. Poulakakis, "Composing limit cycles for motion planning of 3d bipedal walkers," in *2016 IEEE 55th Conference on Decision and Control (CDC)*. IEEE, 2016, pp. 6368–6374.

[8] X. Da, O. Harib, R. Hartley, B. Griffin, and J. W. Grizzle, "From 2d design of underactuated bipedal gaits to 3d implementation: Walking with speed tracking," *IEEE Access*, vol. 4, pp. 3469–3478, 2016.

[9] I. R. Manchester and J. Umenberger, "Real-time planning with primitives for dynamic walking over uneven terrain," in *2014 IEEE International Conference on Robotics and Automation (ICRA)*. IEEE, 2014, pp. 4639–4646.

[10] A. D. Ames, "Human-inspired control of bipedal walking robots," *IEEE Transactions on Automatic Control*, vol. 59, no. 5, pp. 1115–1130, 2014.

[11] A. D. Ames, P. Tabuada, A. Jones, W.-L. Ma, M. Rungger, B. Schürmann, S. Kolathaya, and J. W. Grizzle, "First steps toward formal controller synthesis for bipedal robots with experimental implementation," *Nonlinear Analysis: Hybrid Systems*, vol. 25, pp. 155–173, 2017.

[12] M. J. Powell, A. Hereid, and A. D. Ames, "Speed regulation in 3d robotic walking through motion transitions between human-inspired partial hybrid zero dynamics," in *2013 IEEE International Conference on Robotics and Automation*. IEEE, 2013, pp. 4803–4810.

[13] J. W. Grizzle, C. Chevallereau, A. D. Ames, and R. W. Sinnet, "3d bipedal robotic walking: models, feedback control, and open problems," *IFAC Proceedings Volumes*, vol. 43, no. 14, pp. 505–532, 2010.

[14] E. R. Westervelt, C. Chevallereau, J. H. Choi, B. Morris, and J. W. Grizzle, *Feedback control of dynamic bipedal robot locomotion*. CRC press, 2007.